NANO LETTERS

Letter

pubs.acs.org/NanoLett

Near-Field Radiative Cooling of Nanostructures

Biswajeet Guha,[†] Clayton Otey,[‡] Carl B. Poitras,[†] Shanhui Fan,[‡] and Michal Lipson*[,†,§]

[†]School of Electrical and Computer Engineering, Cornell University, Ithaca, New York 14853, United States

[‡]Ginzton Laboratory, Stanford University, Stanford, California 94305, United States

[§]Kavli Institute at Cornell for Nanoscience, Cornell University, Ithaca, New York 14853, United States

Supporting Information

ABSTRACT: We measure near-field radiative cooling of a thermally isolated nanostructure up to a few degrees and show that in principle this process can efficiently cool down localized hotspots by tens of degrees at submicrometer gaps. This process of cooling is achieved without any physical contact, in contrast to heat transfer through conduction, thus enabling novel cooling capabilities. We show that the measured trend of radiative cooling agrees well theoretical predictions and is limited mainly by the geometry of the probe used here as well as the minimum separation that could be achieved in our setup. These results also pave the way for realizing other new effects based on resonant heat transfer, like thermal rectification and negative thermal conductance.

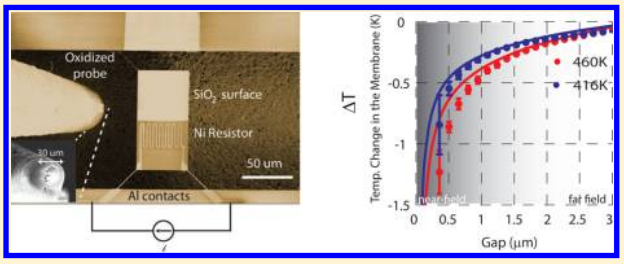

KEYWORDS: *Near-field, thermal radiation, resistive thermometry, cooling*

Heat transfer at a distance through radiation, as opposed to through conduction, is usually thought of as a minuscule effect. It was recently demonstrated that heat transfer through radiation between two surfaces in the near-field regime (i.e., at small enough length scales compared to the characteristic wavelength of thermal radiation which is ~10 μm at 300 K) can be extremely effective and can exceed the traditional heat transfer through radiation in the far-field regime (i.e., blackbody radiation) by several orders of magnitude.[1,3,4] This phenomenon can be used to cool hotspots in thermally isolated nanostructures by coupling local thermal fields to evanescent surface electromagnetic modes of a nearby surface, and rate of cooling would increase dramatically as the separation between the two surfaces reduces. We demonstrate radiative cooling of up to a few degrees and show that in principle this process can efficiently cool down localized hotspots by tens of degrees in sub-100 nm gaps.

Radiative heat transfer between two adjacent surfaces can be resonantly enhanced through the coupling of surface phonon polariton (SPhP) modes,[2,4,5] hybrid surface modes that originate due to resonant coupling between the electromagnetic field and the optical phonons of the material. Surface plasmons in doped Si[6,7] or photonic crystal slabs[8] can lead to a similar effect. Here we choose to work with two SiO_2 surfaces since the SiO_2/air SPhP frequencies (3.5×10^{13} and 1.5×10^{13} Hz) are close to the peak blackbody radiation frequency at room temperature (3.1×10^{13} Hz). Figure 1a shows heat flux as a function of gap between two such parallel SiO_2 surfaces. From Figure 1a, it can be seen that at gaps close to 10 nm, the radiative heat flux is 4 orders of magnitude greater than blackbody radiation. In fact for plates of 1 cm^2 surface area separated by a gap of 50 nm, the radiative thermal conductance is the same as the solid-state conductance of 1 cm^3 copper. Enhanced radiative heat transfer at nanoscale gaps has been measured recently in sphere−plane geometry by optical readout of a bimaterial cantilever[10−12] and also in plane−plane geometry with gaps of up to a few micrometers.[13] In order to observe actual cooling due to near-field radiative heat transfer, the nanostructures have to be sufficiently isolated from its surrounding thermal bath such that the radiative channel becomes the most significant thermalization pathway.

Here we show cooling through radiation of a thermally isolated nanoscale structure by bringing it in proximity (but not in contact) with a probe connected to a thermal bath (see Figure 1b). The nanostructure, acting as the hot spot, is a suspended SiO_2 membrane. Thermal isolation is achieved by connecting the membrane to the substrate using thin spokes, resulting in low background conductance. The 100 × 50 μm membrane is made of SiO_2 that is 840 nm thick and is attached to the silicon substrate using thin spokes that are 600 nm wide and 30 μm long (Figure 2a). XeF_2-based dry etch process was used to release the membrane over a 200 μm trench. The trench was deep enough to ensure that there is negligible spurious coupling of surface electromagnetic modes to the substrate. A 50 nm thick Ni resistor is integrated on top of the membrane with connecting leads through two of the spokes. Al wires connect the resistor to pads which are then wire bonded to a package. A tungsten probe tip (30 μm diameter), coated with 2 μm PECVD SiO_2, is connected to a heat sink, and its background conductance is much higher than that of the

Received: May 6, 2012
Revised: August 8, 2012
Published: August 14, 2012

   dx.doi.org/10.1021/nl301708e | *Nano Lett.* 2012, 12, 4546−4550

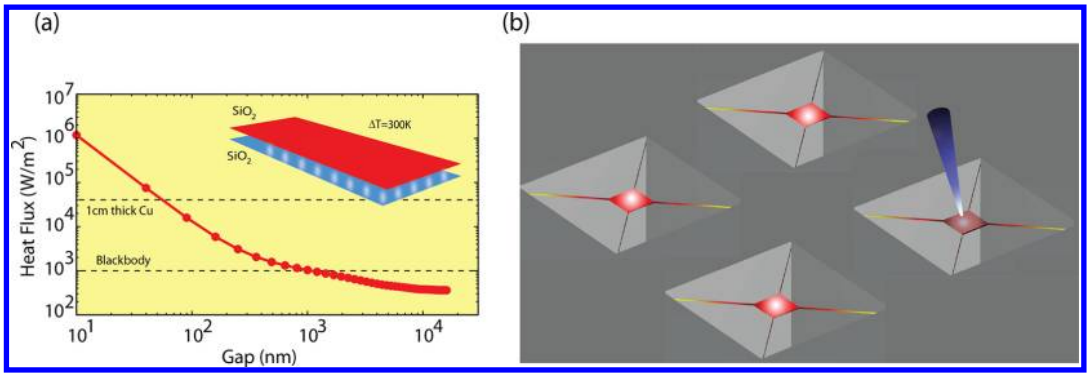

Figure 1. Enhancement of radiative heat transfer in near-field. (a) Radiative heat flux between two SiO_2 surfaces (inset) held at temperatures of 300 K (red surface) and 0 K (blue surface), respectively. (b) Schematic of the experiment where one out of several isolated hotspots is cooled by radiative near-field coupling to a tip.

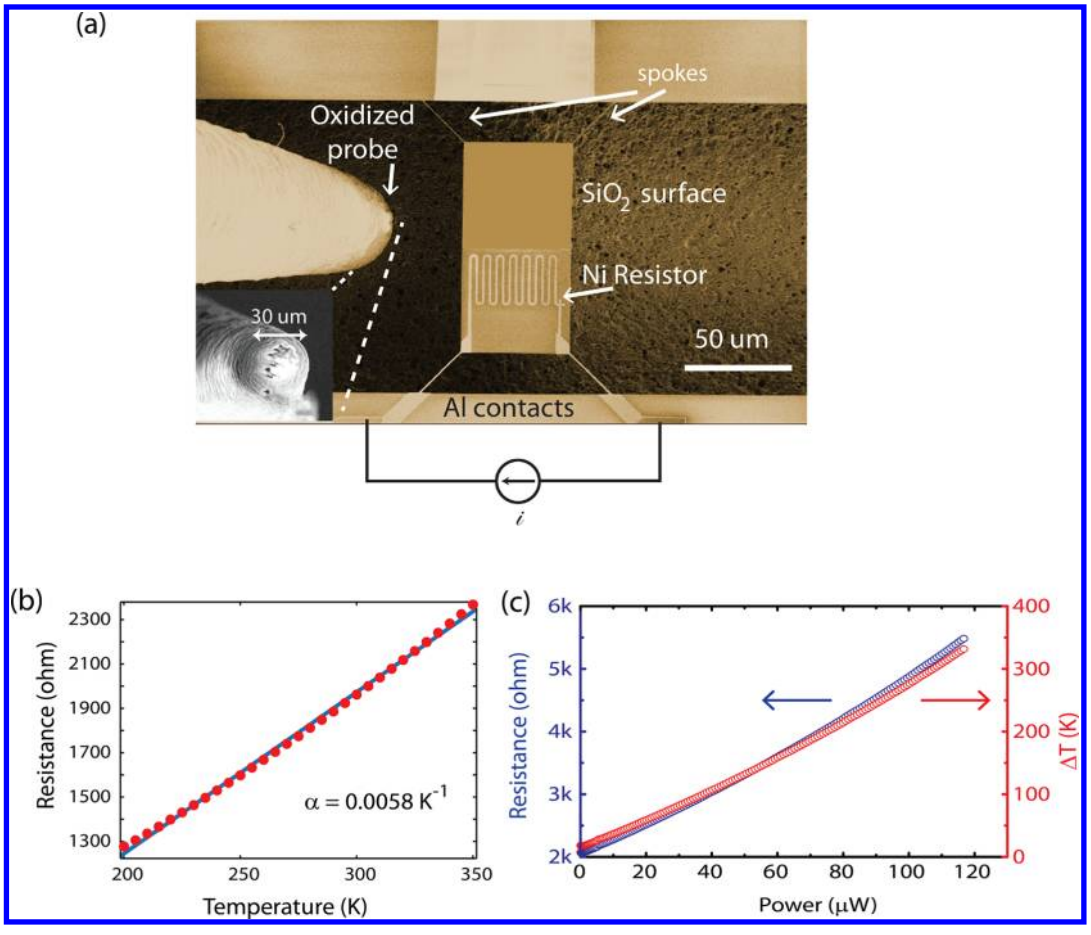

Figure 2. Device characteristics. (a) Top view SEM image of the suspended SiO_2 membrane with integrated resistor and the probe close to it. Inset shows zoom-in of the SiO_2 coated probe tip. (b) Resistance of the Ni resistor over a wide temperature range. The temperature coefficient of resistance was measured to be 0.0058 K^{-1}. (c) Change in resistance measured across the Ni resistor and corresponding temperature increase as power are dissipated in the resistor.

membrane. Figure 2a shows a top view SEM image of the suspended membrane with the probe tip in the inset. All experiments were performed under a vacuum of 10^{-5} Torr, where thermal conduction through air is negligible.

Cooling was measured directly by integrating small resistive thermometers in the hotspots. Resistive thermometry can be extremely sensitive in detecting very small thermal fluxes, especially when used in platforms which are thermally isolated from the environment.[14−16] Thermal isolation also increases the near-field cooling sensitivity, so that radiative heat flux dominates over any other background thermalization pathway. Here Ni thermistors are used to heat the membrane relative to the tungsten tip to an initial temperature T_0 and then monitor the change in temperature of the membrane by monitoring the change in resistance. In order to relate resistance change to temperature change, the temperature sensitivity of the Ni resistor was calibrated beforehand by measuring the resistance over a range of 200−350 K, shown in Figure 2b. The temperature coefficient of resistance $[\alpha = (1/R_0)(\partial R/\partial T)]$ was measured to be 0.0058 K^{-1}. Since the thermal resistance of the

dx.doi.org/10.1021/nl301708e | Nano Lett. 2012, 12, 4546−4550

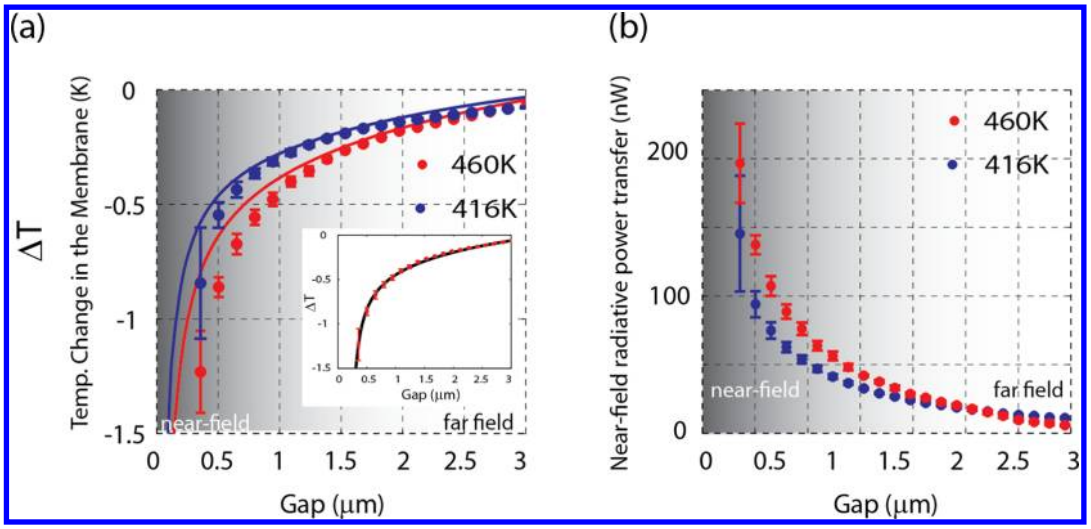

Figure 3. Near-field cooling. (a) Temperature drop due to radiative heat transfer as the probe is brought closer to the membrane, for two different initial membrane temperatures. Error bars represent the standard deviation of each measurement. Solid lines show theoretical prediction. Inset shows fitting of the measured data with model, yielding a gap uncertainty of 160 nm. (b) Near-field power transfer between the membrane and probe as a function of separation.

suspended membrane is much lower than the spokes connecting it to its surrounding, it can be assumed that the temperature of the membrane is almost constant and follows that of the resistor. Very small electrical power is needed to heat up the membrane significantly because of its thermal isolation. Both the resistance and temperature increase of the resistor as a function of the applied DC power are shown in Figure 2c. From the plot one can see that a total power of 30 μW heats the resistor up by 80 K, which corresponds to a background conductance of 360 nW/K. As the probe is brought in proximity to the membrane, the resistance of the heater on the suspended membrane changes due to of the addition of an extra thermalization pathway. The probe is brought closer to the membrane in steps of 350 nm using piezoactuators, and at each gap step the system was allowed to thermally stabilize for 1 min, while the instantaneous power and temperature were monitored. Contact of the probe tip to the surface results in a giant change in resistance, which is used to calibrate the probe membrane separation (see Supporting Information, Figure 6).

We experimentally observe radiative cooling of up to 1.5 K for a separation of 350 nm between the SiO_2 surfaces. Radiative cooling is defined as the decrease in temperature of the membrane from its initial temperature due to radiative coupling.

$$\Delta T(d) = T(d) - T_0 \tag{1}$$

where $\kappa_{rad}(d)$ is the near-field radiative thermal conductance, T_0 is the membrane temperature when the probe is in the far-field, and $T(d)$ is the membrane temperature when the probe is at a separation d. Radiative thermal conductance is defined as $\kappa_{rad}(d) = (P_{rad}(d))/(T_0 - rt)$, where $P_{rad}(d)$ is the near-field radiative power transfer and rt is room temperature. The measured temperature change of the membrane as a function of probe-membrane separation is shown in Figure 3a. It can be seen that when the probe is in the far-field region ($d > 2$ μm), the temperature of the membrane is relatively insensitive to small variations in the distance of the probe from the membrane. As the probe is brought closer to the membrane, the temperature drops due to the near-field coupling. From Figure 3a it can be seen that when the membrane is heated to an initial temperature of 416 K, the temperature drop due to radiative cooling is around 0.8 K. Increasing the temperature gradient leads to larger radiative heat transfer (eq 2), and when the initial temperature is increased to 460 K (up to 160° above room temperature), the radiative temperature drop increases to 1.5 K. The theoretically predicted trend of temperature decrease is shown in solid lines. It agrees well with the measured data, along with a constant offset. This offset is due to uncertainty in gap measurement, which is explained below. Following eq 1, cooling of the membrane due to radiative coupling can be expressed as (see Supporting Information)

$$\Delta T(d + \delta) = \frac{\kappa_{rad}(d)}{\kappa_{rad}(d) + \kappa_{bck}}(T_0 - rt) \tag{2}$$

where κ_{bck} is the background thermal conductance. Background conductance here refers to all other channels (except near-field radiation) through which the membrane can lose heat and includes heat dissipation through the thin supporting spokes and far-field radiation. δ is introduced as a fitting parameter which gives an indication of the uncertainty in gap measurement. κ_{rad} was modeled using a sphere−plane configuration, assuming a 840 nm SiO_2 slab and temperature difference used in the experiment (simulation details in Supporting Information). The resulting electromagnetic heat transfer was calculated numerically using scattering matrix analysis.[17] The far-field component of radiation increases by ∼7% as gap is reduced from 350 to 3500 nm. We have estimated this view factor effect by calculating the absorption by the finite area of the membrane of far-field emission from the sphere. Measured data were fitted to the model using δ and κ_{bck} as fitting parameters. Figure 3a inset shows the resulting fit, with δ = 160 nm and κ_{bck} = 340 nW/K. This value of background conductance agrees well with the expected value of 360 nW/K (see Figure 2c, slope of P vs ΔT). We estimate the gap uncertainty to be relatively small—of the order of 160 nm—and it has several contributing factors, like roughness of the probe tip and slight curvature of the release oxide membrane. Note that the gap uncertainty δ, estimated to be 160 nm, is much smaller than the range of gaps measured (0.3−3.5 μm).

dx.doi.org/10.1021/nl301708e | Nano Lett. 2012, 12, 4546−4550

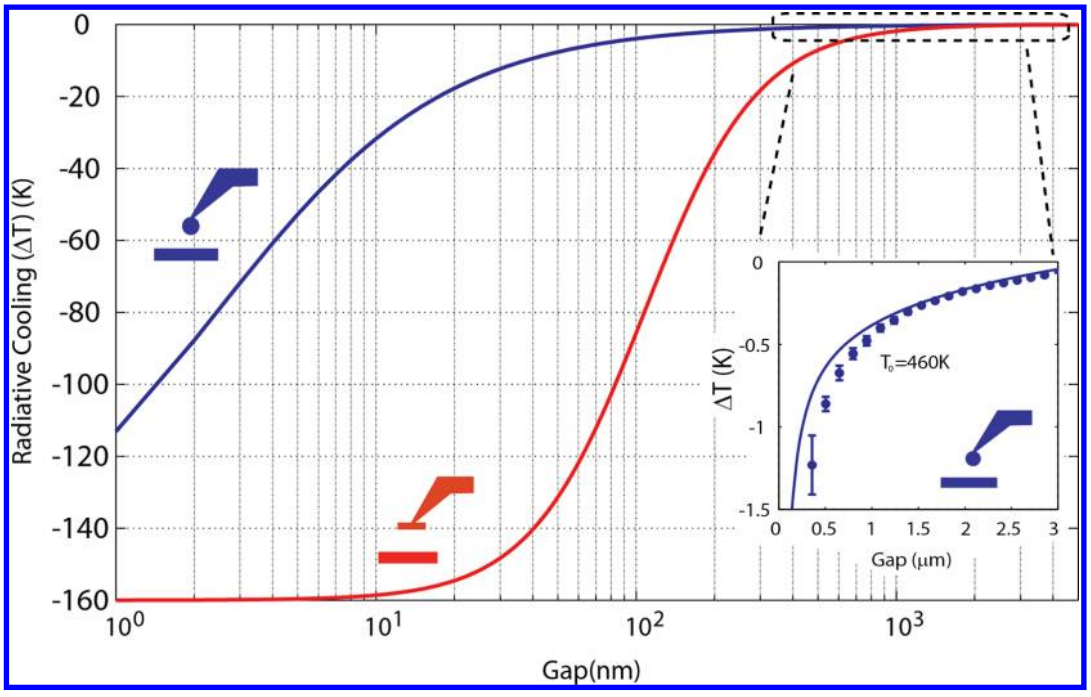

Figure 4. Estimated cooling efficiency. Estimated temperature reduction for a 100 × 50 μm hotspot, using both spherical and planar probes. The spherical probe has a tip diameter of 30 μm. The hotspot has a background conductance of 350 nW/K and is heated to an initial temperature of 160 K. All values are typical of the devices used in our experiments. Inset shows comparison of experimentally observed radiative cooling with the theoretical trend.

From the measurements one can extract the contribution of near-field radiative heat transfer (see eq 2). The increase in the power transfer from the membrane to the probe tip as a function of gap is shown in Figure 3b for various temperature gradients. One can clearly see the signature of enhanced radiative effect for distances below 3 μm.

The measured trend of degree of radiative cooling efficiency agrees well with theoretical predictions and is limited mainly by the geometry of the probe used here as well as the minimum separation that could be achieved in our setup. Figure 4 shows the theoretical temperature decrease of the SiO_2 membrane due to radiative cooling when another surface is brought closer; assuming either a spherical probe with 30 μm tip diameter (similar to the one used in our experiments)[9] or another a parallel SiO_2 surface as a probe. The membrane dimension was assumed to be 100 × 50 μm, same as the one used in our experiments. The background conductance was assumed to be 350 nW/K, which is close to the measured background in our structures. In the simulations the membrane was heated to an initial temperature of 460 K, while the probe was at room temperature. Our calculations are in good agreement with the experimental data (see Figure 4 inset), and cooling by over 20° should be achievable in the sub-50 nm regime using our configuration. While the spherical probe can cool down the membrane by up to 30 K at a gap of 10 nm (blue curve), our calculations show that the near-field effect is even more pronounced when the probe is planar (red curve) and can reduce the temperature by over 100 K at sub-100 nm gaps.

In summary, we demonstrated efficient cooling using near-field radiative heat transfer in a novel platform with temperature sensors integrated directly in thermally isolated hotspots. We measured a local temperature reduction of up to 1.5 K, limited only by geometry and gap resolution, and showed theoretically that it should be possible to achieve very strong cooling in the near-field regime using a modified geometry. This method of thermal management using a noncontact approach could enable cooling when contact methods are not an option, such as in the case of microelectromechanical devices and front-end of microelectronics. This novel platform can also pave the way toward exploring new aspects of radiative heat transfer, such as the recently predicted thermal rectification[18,19] and negative thermal conductance.[20]

■ ASSOCIATED CONTENT

Supporting Information

Detailed fabrication and experimental procedures and theoretical estimation of radiative heat transfer.

This material is available free of charge via the Internet at http://pubs.acs.org.

■ AUTHOR INFORMATION

Corresponding Author

*E-mail: ml292@cornell.edu

Notes

The authors declare no competing financial interest.

■ ACKNOWLEDGMENTS

This material is based upon work supported by the NSF under grant nos. 1002060 and 1143893. The authors also gratefully acknowledge support from DARPA for award no. W911NF-11-1-0435 supervised by Dr. Jagdeep Shah. This work was performed in part at the Cornell Nanoscale Facility (a member of the National Nanofabrication Users Network) which is supported by National Science Foundation (grant ECS-0335765), its users, Cornell University, and Industrial Affiliates. We would like to acknowledge NSF and Cornell Center for Nanoscale Systems (CNS, NSF award no. EEC-0117770, 0646547, and the New York State Office of Science,

Technology & Academic Research under NYSTAR contract no. C020071). C.O. and S.F. acknowledge the support of an AFOSR-MURI program (grant no. FA9550-08-1-0407). The authors thank M. Soltani and S. Shivaraman for helpful discussions.

REFERENCES

(1) Pendry, J. Radiative exchange of heat between nanostructures. *J. Phys.: Condens. Matter* **1999**, *11*, 6621.
(2) Mulet, J. P.; Joulain, K.; Carminati, R.; Greffet, J. J. Nanoscale radiative heat transfer between a small particle and a plane surface. *Appl. Phys. Lett.* **2001**, *78*, 2931.
(3) Polder, D.; Vanhove, M. Theory of Radiative Heat Transfer between Closely Spaced Bodies. *Phys. Rev. B* **1971**, *4*, 3303−3314.
(4) Volokitin, A.; Persson, B. Near-field radiative heat transfer and noncontact friction. *Rev. Mod. Phys.* **2007**, *79*, 1291−1329.
(5) Basu, S.; Zhang, Z.; Fu, C. Review of near-field thermal radiation and its application to energy conversion. *Int. J. Energy Res.* **2009**, *33*, 1203−1232.
(6) Fu, C. J.; Zhang, Z. M. Nanoscale radiation heat transfer for silicon at different doping levels. *Int. J. Heat Mass Tran.* **2006**, *49*, 1703−1718.
(7) Rousseau, E.; Laroche, M.; Greffet, J. J. Radiative heat transfer at nanoscale mediated by surface plasmons for highly doped silicon. *Appl. Phys. Lett.* **2009**, *95*, 231913.
(8) Ben-Abdallah, P.; Joulain, K.; Pryamikov, A. Surface Bloch waves mediated heat transfer between two photonic crystals. *Appl. Phys. Lett.* **2010**, *96*, 143117.
(9) Kittel, A.; Hirsch, W. M.; Parisi, J.; Biehs, S.; Reddig, D.; Holthaus, M. Near-field heat transfer in a scanning thermal microscope. *Phys. Rev. Lett.* **2005**, *95*, 224301.
(10) Narayanaswamy, A.; Shen, S.; Chen, G. Near-field radiative heat transfer between a sphere and a substrate. *Phys. Rev. B* **2008**, *78*, 115303.
(11) Rousseau, E.; Siria, A.; Jourdan, G.; Volz, S.; Comin, F.; Chevrier, J.; Greffet, J. J. Radiative heat transfer at the nanoscale. *Nat. Photonics* **2009**, *3*, 514−517.
(12) Shen, S.; Narayanaswamy, A.; Chen, G. Surface Phonon Polaritons Mediated Energy Transfer between Nanoscale Gaps. *Nano Lett.* **2009**, *9*, 2909−2913.
(13) Ottens, R. S.; Quetschke, V.; Wise, S.; Alemi, A. A.; Lundock, R.; Mueller, G.; Reitze, D. H.; Tanner, D. B.; Whiting, B. F. Near-Field Radiative Heat Transfer between Macroscopic Planar Surfaces. *Phys. Rev. Lett.* **2011**, *107*, 014301.
(14) Kim, P.; Shi, L.; Majumdar, A.; McEuen, P. L. Thermal transport measurements of individual multiwalled nanotubes. *Phys. Rev. Lett.* **2001**, *87*, 215502.
(15) Schwab, K.; Henriksen, E. A.; Worlock, J. M.; Roukes, M. L. Measurement of the quantum of thermal conductance. *Nature* **2000**, *404*, 974−977.
(16) Tighe, T. S.; Worlock, J. M.; Roukes, M. L. Direct thermal conductance measurements on suspended monocrystalline nanostructures. *Appl. Phys. Lett.* **1997**, *70*, 2687.
(17) Otey, C.; Fan, S. Numerically exact calculation of electromagnetic heat transfer between a dielectric sphere and plate. *Phys. Rev. B* **2011**, *84*, 245431.
(18) Otey, C.; Lau, W. T.; Fan, S. Thermal Rectification through Vacuum. *Phys. Rev. Lett.* **2010**, *104*, 154301.
(19) Basu, S.; Francoeur, M. Near-field radiative transfer based thermal rectification using doped silicon. *Appl. Phys. Lett.* **2011**, *98*, 113106.
(20) Zhu, L.; Otey, C.; Fan, S. Negative differential thermal conductance through vacuum. *Appl. Phys. Lett.* **2012**, *100*, 044104.